

Expanding the Biocatalytic Toolbox with a New Type of ene/yne-Reductase from *Cyclocybe aegerita*

Dominik Karrer,^[a] Martin Gand,^[a] and Martin Rühl^{*,[a, b]}

This study introduces a new type of ene/yne-reductase from *Cyclocybe aegerita* with a broad substrate scope including aliphatic and aromatic alkenes/alkynes from which aliphatic C8-alkenones, C8-alkenals and aromatic nitroalkenes were the preferred substrates. By comparing alkenes and alkynes, a ~2-fold lower conversion towards alkynes was observed. Furthermore, it could be shown that the alkyne reduction proceeds via a slow reduction of the alkyne to the alkene followed by a rapid reduction to the corresponding alkane. An accumulation of the

alkene was not observed. Moreover, a regioselective reduction of the double bond in α,β -position of $\alpha,\beta,\gamma,\delta$ -unsaturated alkenals took place. This as well as the first biocatalytic reduction of different aliphatic and aromatic alkynes to alkanes underlines the novelty of this biocatalyst. Thus with this study on the new ene-reductase CaeEnR1, a promising substrate scope is disclosed that describes conceivably a broad occurrence of such reactions within the chemical landscape.

Introduction

Regarding the principles and metrics of green chemistry, waste prevention, atom efficiency, reduction of hazardous materials, harmless solvents and auxiliaries, energy efficiency, use of renewable raw materials, shorter synthesis routes (avoiding derivatization), use of catalytic rather than stoichiometric reagents, analytics for pollution prevention and inherently safer processes are core points.^[1] Biocatalytic approaches can fulfill these principles. Therefore, interdisciplinary collaborations in the field of biotechnology, molecular biology and biochemistry achieved major advances in this field in the recent decades. Recently, the ACS Green Chemistry Institute's Pharmaceutical Round Table (GCIPR) defined ten key research areas including among others the asymmetric hydrogenation of olefins/enamines and imines, displaying the importance of novel biocatalysts reducing multiple carbon-carbon bonds.^[2] Enzymes capable to reduce such carbon bonds, collectively known as ene-reductases (ERs) have been studied intensely throughout the last decades. The physiological importance of ERs is broadly defined, which includes among others, detoxification of compounds derived from lipid peroxides in plants, quinone

accumulation in yeast or the putative involvement in various biosynthetic pathways such as the modification of lipoxygenase-derived C8-oxylinols displaying a vast variability in their biological importance.^[3,4,5,6,7] This variability agitated a lot of attention concerning biocatalytic approaches like the production of bioactive compounds, pharmaceuticals, agricultural chemicals or chiral building blocks.^[4] The most prominent family of ERs are the flavin mononucleotide (FMN) depending Old Yellow Enzymes (OYEs) which reduce multiple α,β -unsaturated aldehydes, ketones, esters or nitro compounds.^[8–10] Due to significant advances in protein engineering strategies, OYEs have been successfully employed to improve their catalytic activities, invert stereoselectivities, broaden the substrate scope or even catalyze a variety of unusual reductions with a high value for industrial approaches (Figure 1).^[11] Furthermore, the application of ERs with novel reduction capabilities due to site-directed mutagenesis or by implementing ERs in biocatalytic

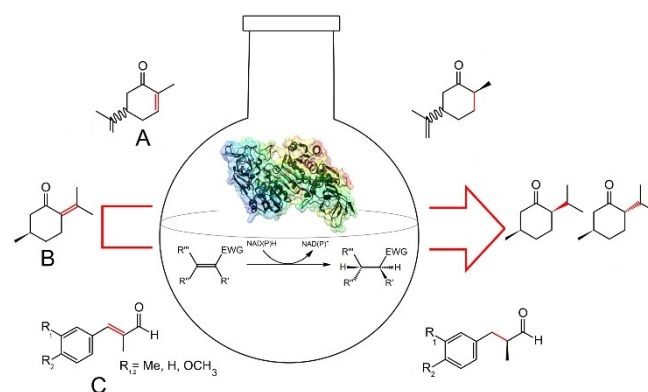


Figure 1. Reactions catalyzed by various ERs (A) OYE from *Synechococcus* sp. PCC 7942 reducing carvone to a key intermediate in striatinic and pechuloic acid production. (B) MDR from *Mentha piperita* reducing (+)-pulegone to (–)-menthone and (+)-isomenthone. (C) OYE1-3 from *Lycopersicon esculentum* reducing cinnamaldehyde-like substrates to fragrances.

[a] D. Karrer, Dr. M. Gand, Dr. M. Rühl
Department of Biology and Chemistry
Justus-Liebig University Giessen
Institute of Food Chemistry and Food Biotechnology
35392 Giessen (Germany)
E-mail: martin.ruehl@uni-giessen.de

[b] Dr. M. Rühl
Fraunhofer Institute for Molecular Biology and Applied Ecology IME Business
Area Bioresources
35392 Giessen (Germany)

Supporting information for this article is available on the WWW under
<https://doi.org/10.1002/cctc.202002011>

© 2021 The Authors. ChemCatChem published by Wiley-VCH GmbH. This is an open access article under the terms of the Creative Commons Attribution Non-Commercial NoDerivs License, which permits use and distribution in any medium, provided the original work is properly cited, the use is non-commercial and no modifications or adaptations are made.

cascades to replace traditional synthetic steps is obviously popular and constantly increasing.^[3,4] Although ERs are studied extensively, their interest in sustainable and green chemistry is still rising and exemplifies the need of an increasing biocatalytic landscape filled with a broad range of biocatalysts for more and more tailored and “new-to-nature” C=C or C≡C containing compounds.^[11]

On closer consideration of currently known ERs, several structures with C=C bonds can be reduced but a variable biocatalyst that is also able to perform a “new-to-nature”-like reduction of C≡C bonds has only been shown once for solely one compound. Due to the prevalence of activated alkynes, organic chemists extensively investigated efficient methods for their reduction. The most common strategies include the use of transition metal catalysts to produce saturated products. It has been reported that aromatic and aliphatic alkynes were successfully reduced by using Pd/C or Pd-dibenzylideneacetone catalysts.^[12,13] More recently, quantitative hydrogenations towards two aliphatic alkynes were accomplished with a methyl-substituted phosphatane oxide catalyst in the presence of organosilanes as the terminal reductant.^[14] An alternative method to reduce aliphatic alkynes was shown with an iridium (III)-complex as catalyst.^[15] In general, these methods do not meet all of the mentioned green and sustainable chemistry standards, due to their inevitable use of costly transition-metal catalysts.^[1] Furthermore, the synthesis of such catalysts often require various additional synthetic steps.^[16,17] To our knowledge, these reductions are mostly limited to alkynoates, meaning that reports of the reduction of alkynals and alkynones are scarce. Taken together, the biocatalytic landscape lacks a reductase targeting C≡C bonds that opens up an uncovered field of biocatalysis. To overcome this issue, focusing on other types of ERs or targeting other organisms than bacteria, plants or baker's yeast could be productive. Regarding other types of ERs, the flavin adenine dinucleotide (FAD)- and [4Fe-4S]-depending ERs, the NAD(P)H-dependent medium-chain dehydrogenase/reductase superfamily (MDR) as well as the NAD(P)H-dependent short-chain dehydrogenase/reductase superfamily (SDR) are far less studied for biocatalytic applications.^[5,10,18,19,20]

An evaluation of their biocatalytic potential is almost lacking. Regarding other organisms, a promising portfolio of ERs with novel activities was shown via whole cell biotransformations of α,β -unsaturated substrates in various fungi from the phyla Ascomycota and Basidiomycota.^[21,22] This implicates a huge enzyme library with great potential in substituting conventional synthesis with environmentally friendly biocatalysts. So far, only one study targeted an ER from the yeast-like Basidiomycota *Sporidiobolus salmonicolor* that reduced unnatural large monocyclic enones like (*E*)-3-methylcyclopentadec-2-en-1-one, cyclopentadec-2-en-1-one, and cyclododec-2-en-1-one to their corresponding saturated ketones.^[23] Hence, this study investigated the biocatalytic value of the first ER from a filamentous fungi of the phylum Basidiomycota as a member of the MDR-superfamily. This ER turned out to exhibit novel biocatalytic activities displaying a valuable and versatile biocatalyst with high potential for future approaches.

Results and Discussion

Biochemical characterization and cofactor specificity

Following heterologous production in *E. coli* and purification, the effects of pH and temperature on CaeEnR1 (accession number: MW013782, AAE3_13549 www.thines-lab.senckenberg.de/agrocybe_genome) activity was determined with oct-1-en-3-one (**1**) as substrate. CaeEnR1 showed maximum activity at pH 7.5 with more tolerance against acidic conditions. 50% of its activity left at pH 5.0 that increased with higher pH-values. Decreasing and increasing values (pH < 5 or > 7.5) resulted in a drastic loss of activity with ~25% left at pH 4.5 and < 10% at pH 8–10 (Figure 2A). CaeEnR1 showed maximum activity at 25–30°C. Increasing temperatures resulted in a steady loss with no activity left at 50°C. A low temperature of 4°C led also to a suppression of enzyme activity (Figure 2B).

Cofactor specificity with **1** as substrate was determined with NADPH and NADH, revealing a > 700-fold higher preference for NADPH with 28.0 U·mg⁻¹ compared to NADH with

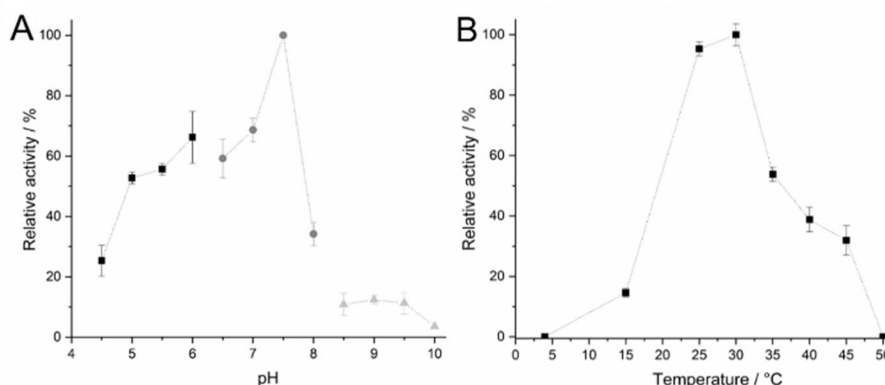


Figure 2. Influence of pH (A) (squares = 50 mM acetate buffer, circles = 50 mM phosphate buffer, triangles = 50 mM borate buffer) and of temperature (B) on CaeEnR1 activity.

0.04 U·mg⁻¹. Other ene-reductases from the MDR-superfamily as NtDBR (> 1,600-fold) or SsERD (no activity with NADH) also prefer NADPH as hydride donor.^[23,24] This is not surprising, due to the fact that these enzymes share several amino acids, such as G189, K193 and Y208, which were shown to be involved in NADPH binding by the crystal structures of NtDBR and AtDBR (Supporting information Figure S1A, B).^[4,20]

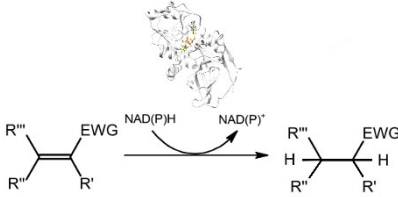
Reduction of alkenals and alkenones

To explore the substrate profile of CaeEnR1, the conversion rates (Table 1) of in total 21 different alkenals and alkenones were examined. These substrates were grouped according to their structure and physicochemical properties: aliphatic α,β -unsaturated alkenones: oct-1-en-3-one (1), oct-3-en-2-one (2), hex-1-en-3-one (3) (group I); aliphatic α,β -unsaturated alkenals: (*E*)-oct-2-enal (4), (*E*)-non-2-enal (5), (*E*)-hex-2-enal (6) (group II); aliphatic $\alpha,\beta,\gamma,\delta$ - and multiple- unsaturated alkenals: (*E,E*)-oct-2,4-dienal (7), (*E,E*)-non-2,4-dienal (8) (*E,E*)-non-2,6-dienal (9)

(group III); α,β -unsaturated alcohols: oct-1-en-3-ol (10), oct-2-en-1-ol (11) (group IV); cyclic α,β -unsaturated alkenones/alkynones: (*R,S*)-carvone (12), β -damascenone (13), 1,2-naphthoquinone (14), 4-phenyl-3-butene-2-one (15) (group V); cyclic α,β -unsaturated alkenals: coniferyl aldehyde (16), cinnamaldehyde (17), 2-phenyl-but-2-enal (18), β -cyclocitral (19) (group VI); cyclic α,β -unsaturated nitroalkenes: (*E*)- β -nitrostyrene (20), (*E*)- β -methyl- β -nitrostyrene (21) (group VII). Most conversion rates of group I and group II showed rates of up to 72% - 98%; only 2 and 6 were converted by 48% and 54%, respectively. While the conversion rates of group III showed values of up to 73% - 84% (Table 1). Remarkably, CaeEnR1 reduced selectively the double bond in α,β -position of 7, 8 and 9. However, no successful reduction of the substrates from group IV was detected. Compounds 15 (50%) and 17 (59%) were the only converted substrates of group V and VI, respectively. Related structures like 16 or 18 were either very poorly or not converted (Table 1).

This could be caused by steric effects of the methyl group adjacent to the double bond. Compared to 17, 16 has an additional phenolic hydroxy- and methoxy group, implicating

Table 1. Reduction of various activated alkenals/alkenones by CaeEnR1. A typical reaction mixture (1 mL) contained 0.2 mM NADPH, 0.1 mM substrate and 5 μ M CaeEnR1 in 50 mM phosphate buffer (pH 7.5). The reactions were incubated at 24 °C for 3 h at 160 rpm. CaeEnR1 did not catalyze the reduction of the substrates: oct-1-en-3-ol (10), oct-2-en-1-ol (11), (*R,S*)-carvone (12), β -damascenone (13), 2-phenyl-but-2-enal (18), β -cyclocitral (19).

					
Group	Substrate	Product	Conversion [%]		
I	1	1b	98		
	2	2b	48		
	3	3b	95		
II	4	4b	86		
	5	5b	72		
	6	6b	54		
III	7	7b	73		
	8	8b	84		
	9	9b	27		
VI	15	15b	50		
VII	16	16b	3		
	17	17b	59		
	20	20b	90		
VIII	21	rac-21b	26		

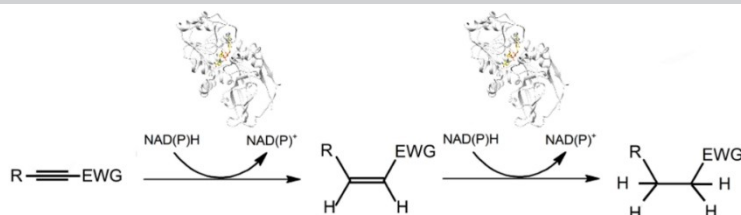
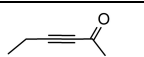
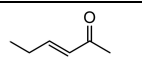
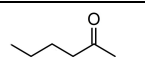
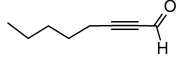
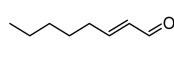
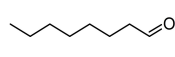
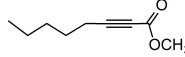
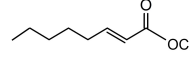
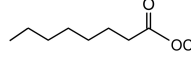
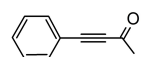
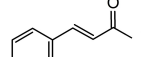
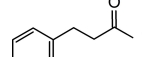

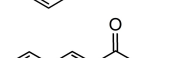
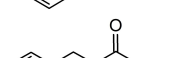



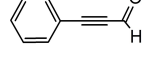
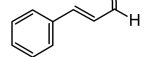
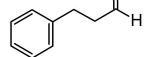
the necessity of an increased substrate tunnel or binding pocket. Possible steric effects were also observed for substrates of group VII. The non-substituted **20** was converted with good rates of 90%, whereas for **21** that contains a methyl group nearby the double bond a conversion of only 26% was achieved. A constriction due to bulky amino acid residues could explain the difference in conversion between substituted and non-substituted aromatic substrates. This was already pointed out for NtDBR, which reduced **17** and **21** with high conversion rates (100% and 71%) while **16**, similar to our study, was poorly reduced (~6%).^[20] The phenylalanine/serine substitution (NtDBR to AtDBR F285/S287, corresponding to S283 in CaeEnR1) was identified as potentially size restricting, allowing AtDBR to reduce substituted cinnamaldehyde-like substrates more efficiently. Especially, F285 in NtDBR was considered as the determinant for the limited reduction of substituted cinnamaldehyde-like substrates.^[4,20] Compared to NtDBR, CaeEnR1 harbors a serine (S283) at that position (Supporting Information S1) similar to AtDBR but shows very poor activity towards **16**, which indicates that this amino acid might not be the responsible determinant for the poor activities towards substituted cinnamaldehyde-like substrates. Furthermore, an efficient and regioselective reduction of the $\alpha,\beta,\gamma,\delta$ -unsaturated aldehydes has not been pointed out so far (Table 1).

In general, CaeEnR1 showed the highest activities towards C8-alkenones and C8-alkenals among aliphatic substrates. With decreasing chain length, a ~2-fold loss was detected (Figure 3A). By comparing the aromatic substrates, the alkenone **15** and alkenal **17** were converted similarly while the nitroalkene counterpart **20** showed drastically higher conversion rates suggesting a higher activation of the C=C bond leading to a better conversion (Figure 3A).

Reduction of alkynals, alkynones and alkynoates

The reduction of alkynals, alkynones and alkynoates were examined by seven different substrates, divided in the two groups of aliphatic (group VIII): hex-3-yn-2-one (**22**), oct-2-ynal (**23**), methyl-oct-2-ynoate (**24**) and aromatic (group IX): 4-phenylbut-3-yn-2-one (**25**), methyl-3-phenylprop-2-ynoate (**26**), 3-phenylprop-2-ynal (**27**), 1-phenyl-2-propyn-1-one (**28**) compounds. CaeEnR1 successfully reduced the aliphatic and aromatic alkynals/alkynones **22**, **23**, **25**, **27** and **28** to their corresponding alkanals and alkanones (Table 2). While **23** showed a satisfactory conversion rate of 42%, the alkynoate counterpart **24** was not reduced to the corresponding alkanoate. Similarly, the aromatic alkynes **25**, **26** and **27** were differently converted depending on their carbonyl species. While the alkynone and alkynal **25** and **27** were converted by

Table 2. Reduction of various activated alkynals/alkynones by CaeEnR1. A typical reaction mixture (1 mL) contained 0.2 mM NADPH, 0.1 mM substrate and 5 μ M CaeEnR1 in 50 mM phosphate buffer (pH 7.5). The reactions were incubated at 24 °C for 3 h at 160 rpm.

								
Substrate	unsat. Product	sat. Product	Total conv. [%]	selectivity [%] alkene	selectivity [%] alkane			
22		22 a		22 b		5	< 0.1	< 99.9
23		4		4 b		42	5	95
24		24 a		24 b		-	-	-
25		15		15 b		22	5	95
26		26 a		26 b		< 1	< 1	< 1
27		17 a		17 b		20	< 1	< 99
28		28 a		28 b		5	< 1	< 99

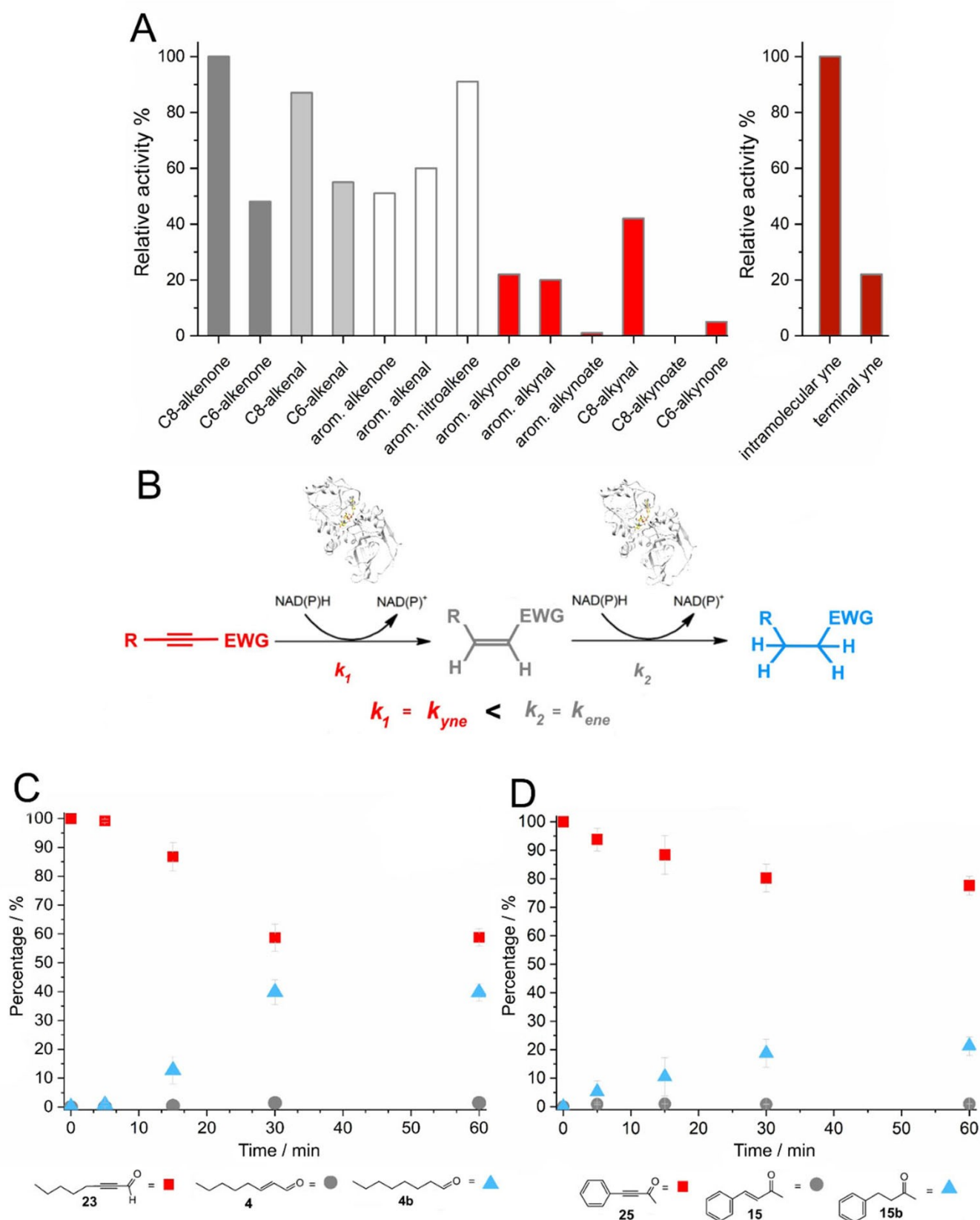


Figure 3. Time dependent reduction of alkynals/alkynones and comparison of the relative activity between alkenes and alkynes depending on chain length, electron withdrawing group and position of the unsaturated bond. (A) Comparison of the relative activities of CaeEnR1 towards various substrate types differing in chain length, carbonyl species and position of the unsaturated alkyne. (B) Two step reduction process with k_1 (alkyne reduction to the alkene), followed by k_2 (alkene reduction to the alkane). Reduction of **23** (C) and **25** (D) to their corresponding alkenals/alkenones **4**, **15** and alkanals/alkanones **4b**, **15b** with standard reaction conditions. Red square = alkyne, grey circle = alkene, blue triangle = fully saturated product.

Table 3. Steady-state kinetics of CaeEnR1 with alkenes. Given values are means \pm of triplicates.

Group	substrate	K_M [μM]	k_{cat} [s^{-1}]	k_{cat}/K_M [$\text{s}^{-1} \cdot \mu\text{M}^{-1}$]
I	1	75.8 \pm 20.8	213.0 \pm 25.6	2.8 \pm 1.0
	2	72.1 \pm 28.9	64.7 \pm 9.2	0.9 \pm 0.3
	3	27.9 \pm 3.2	4.0 \pm 0.2	0.1 \pm 0.1
II	4	211.2 \pm 61.2	41.1 \pm 5.1	0.2 \pm 0.1
	5	180.5 \pm 29.5	10.2 \pm 1.0	0.1 \pm 0.0
	6	n.d.	0.8 \pm 0.2 ^a	n.d.
III	7	n.d.	0.5 \pm 0.1 ^[a]	n.d.
	8	n.d.	1.0 \pm 0.1 ^[a]	n.d.
	9	n.d.	0.8 \pm 0.2 ^[a]	n.d.
VI	14	n.d.	1.2 \pm 0.8 ^a	n.d.
VI	15	120.2 \pm 55.2	34.3 \pm 11.1	0.3 \pm 0.20
VIII	23	n.d.	1.0 \pm 0.4 ^[a]	n.d.
IX	25	n.d.	0.9 \pm 0.4 ^[a]	n.d.

[a] = rates (s^{-1}) with 0.25 mM substrate due to limited solubility of the substrates, significant absorption at 340/365 nm at higher concentrations or near zero-order kinetics. n.d., not determined. Other substrates were not reduced under steady-state conditions.

20–22%, the alkynoate **26** showed a conversion rate under 1% (Table 2).

Furthermore, the alkynoate **28** with a terminal alkyne group was poorly converted with 5% (Table 2). Collectively all reductions of the triple bond lead to minimum amounts (max. 2%) of the alkene intermediate (**22a**, **4**, **15**, **27a**, **28a**) (Table 2). The reduction of the alkynone **25** was so far only described for OYE3.^[26] Generally, the successful reduction of alkynals and alkynones depicts a unique characteristic of CaeEnR1 among other described ERs. Compared to the tested alkenones and alkenals **4**, **15** and **17**, CaeEnR1 showed a \sim 2-fold lower conversion rate towards the alkyne counterparts **23**, **25** and **27** (Figure 3A). Similar observations were made for the aromatic alkenone and alkenal **15**, **17** and their counterparts **25**, **27** (Figure 3A). Furthermore, for compounds with an ester as electron withdrawing group (**24**, **26**) very poor or no conversions were detected. In addition, the position of the triple bond also seems to have a drastic impact on conversion. A \sim 5-fold difference in relative activity between the intramolecular alkyne in **25** and the terminal alkyne in **28** was detected (Figure 3A). To clarify whether the alkynes are first reduced to the corresponding alkene leading to its accumulation followed by the reduction to the fully saturated product, the reduction in a time lap of 60 min exemplarily for **23** and **25** was investigated (Figure 3C, D). Time dependent reduction of alkynals and alkynones revealed that the conversion rates were decent for **23** and **25** with \sim 40% and \sim 20% after 30 min, respectively (Figure 3). **22** was converted very poorly, showing a maximum after 30 min of only \sim 6%. However, the corresponding

alkenals/alkenones (**15**, **4** and **22a**) never exceeded $< 2\%$. This suggests a rapid two-step mechanism including the reduction of the triple bond, leading to the alkenal/alkenone which is instantly further reduced to the saturated product. This is reasonable by comparing the reaction rates and specific activities against the alkynals/alkynones **23/25** and their alkenals/alkenones **4/15** differing by multiple magnitudes (Table 1 and 3). OYE3 from *S. cerevisiae* is also able to reduce **25**. However, this enzyme shows a higher affinity towards the alkyne, which first of all leads to an accumulation of the alkenone followed by a subsequent reduction to the alkanone.^[26]

Preparative scale biotransformation

For biotransformation in a preparative scale, **1** was used as a model substrate with a concentration of 25 mM. Reactions were carried out by using a NADP⁺/glucose dehydrogenase (GDH) recycling system as a source for NADPH. Within 1 h about $\sim 30\%$ of **1** was reduced to the corresponding product **1b**. With ongoing reaction, the percentage of **1b** plateaued at $\sim 40\%$ in the reaction mixture. No further reduction of **1** was detected after 6 h and 16 h (Figure 4). By comparing the conversion rates between the analytical and preparative scale reduction of **1**, a ~ 2.5 -fold difference was noticed (Table 1, Figure 4). Due to the limited solubility of **1**, the solvent percentage was increased from 0.1% (analytical scale) to 10% (preparative scale) ethanol, which might have influenced the activity of CaeEnR1. Further-

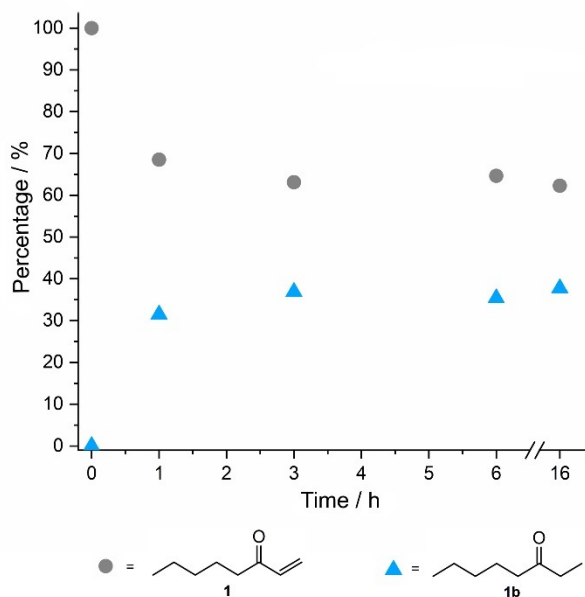


Figure 4. Time dependent reduction of substrate **1** (grey circles) to the corresponding product **1b** (blue triangles) in a preparative scale biotransformation. The reaction was monitored over 16 h at different time points.

more, it has to be noticed that several aspects and problems like heat transfer, transport phenomena, mass balance, proper mixing or the mentioned increasing amounts of organic solvents with higher substrate concentrations arise when it comes to sufficient up-scaling of biotransformations.^[30,31] Nevertheless, a promising first preparative scale biotransformation with CaeEnR1 was demonstrated.

Enzyme kinetics

Kinetic analysis revealed that the affinity of CaeEnR1 differed strongly between α,β -unsaturated ketones, α,β -unsaturated aldehydes and aromatic ketones (Table 3). In some cases (6, 7, 8, 9, 10, 11, 12, 13, 14, 16, 17, 18, 19, 20, 21, 22, 24, 26, 27), full steady-state kinetics were not determined due to either limited solubility, significant absorption at 340/365 nm, near zero-order kinetics or activity under the detection limit. However, the k_{cat} values with 0.25 mM of these substrates were calculated and ranged between 0.5–1.2 s⁻¹ (Table 3). All together, the aliphatic ketones were strongly preferred substrates with K_{M} values between 27.9–75.8 μM which are 2–3 times higher affinities compared to aldehydes (K_{M} =180.5–211.2 μM). Interestingly, $\alpha,\beta,\gamma,\delta$ -unsaturated aldehydes with the same chain length compared to the tested α,β -unsaturated aldehydes showed presumable lower affinities (Table 3). In addition, a high affinity (K_{M} =120.2 μM) and reaction rate (34.3 s⁻¹) towards the aromatic compound **15** was calculated. Surprisingly, **3** showed the lowest K_{M} with 27.9 μM among all tested substrates while the aldehyde analogue **6** showed lower reaction rates and assumingly shows a higher K_{M} . Furthermore, k_{cat} and $k_{\text{cat}}/K_{\text{M}}$ values of α,β -unsaturated substrates, particularly the ketones with eight

carbons were higher compared to the aldehydes and ketones with nine or six carbons (Table 3). The K_{M} values for **4** and **8** are similar with a slightly higher k_{cat} for **4**. With decreasing chain length of the aldehydes, the enzyme activity decreased as well, which suggests a correlation between chain length and affinity. Interestingly, the opposite was observed with α,β -unsaturated ketones, where CaeEnR1 showed the highest affinity towards **3** but coincidentally the lowest k_{cat} and $k_{\text{cat}}/K_{\text{M}}$ values compared to **1** and **2**. Similar findings were observed for AtDBR from *A. thaliana* that shows strikingly lower K_{M} values for α,β -unsaturated aldehydes with longer carbon chains (non-2-enal 5.9 μM , hex-2-enal 232 μM , pent-2-enal 1,420 μM).^[5] Another ER with strikingly lower affinities towards aliphatic substrates like **1** and **5** has been shown for NtDBR.^[20] To our knowledge, AtDBR is the only MDR-superfamily related enzyme that showed activity towards naphthoquinones like **14**.^[25] On consideration of the bioinformatic analysis, AtDBR and CaeEnR1 share the serine residue located in the binding pocket/substrate entrance (Supporting Figure S1B), suggesting that this residue could be crucial for 1,2-naphthoquinone reduction.

Conclusion

Despite their overall potential, research on new biocatalysts from promising specimens of the phyla Basidiomycota is underrepresented. Hence, the first ER from a fungus of the phylum Basidiomycota with high activities towards aliphatic and aromatic α,β -unsaturated compounds was comprehensively characterized. Compared to the very few known ERs of the MDR-superfamily, CaeEnR1 exhibited highly efficient and regioselective reductions of $\alpha,\beta,\gamma,\delta$ -unsaturated aldehydes and is able to reduce activated alkynes to their saturated compounds. This first report on such biocatalytic reductions underlines the uniqueness of CaeEnR1. Collectively, this study introduces a new type of ER with a broad substrate scope including aliphatic and aromatic alkenals/alkenones, alkynals/alkynones and aromatic nitro alkenes. Moreover, the discovery of alkyne reduction and future investigations of the reaction mechanism will also have an impact on “new-to-nature” reactions like the recently described photocatalytic deacetoxylation by MDR-related ERs. For the development of such reactions, knowledge about the mechanism of C=C reductions was crucial.^[28] Furthermore, with this ene/yne-reductase the biocatalytic gap of C \equiv C reductions is filled, which enables a new field of opportunities and challenges for protein engineering approaches, aiming for novel biocatalytic cascades or enzyme improvement via co-factor recycling systems.

Experimental Section

Cloning and protein expression of CaeEnR1

The codon optimized *ENR1* gene (accession number: MW013782, AAE3_13549 www.thines-lab.senckenberg.de/agrocybe_genome) was commercially purchased and cloned into the plasmid pET28a (BioCat GmbH, Heidelberg, Germany). For protein expression,

pET28a/CaeEnR1 plasmid was transformed into *E. coli* BL21 Gold (DE3). *E. coli* cells were cultivated in Terrific Broth medium (TB) containing 12 g tryptone, 24 g yeast extract and 5 g glycerol, supplemented with an equivalent of 1x TB-salts from a 10x stock solution (0.17 M KH_2PO_4 and 0.72 M K_2HPO_4) and 50 $\text{mg}\cdot\text{L}^{-1}$ kanamycin as selection marker at 37 °C until an OD_{600} of 0.4–0.6 was reached. Expression was induced by adding isopropyl- β -D-thiogalactopyranoside to a final concentration of 0.1 mM. Cultivation was continued for another 24 h at 24 °C. Cells were harvested by centrifugation (4,000 g, 30 min, 4 °C) and stored at –20 °C until further use or directly processed.

Protein purification

The cell pellet was thawed on ice and resuspended in lysis-buffer (50 mM phosphate, 300 mM NaCl, 20 mM imidazole, pH 7.5). Disruption of cells was carried out by sonification (3 cycles for 60 s on, 60 s rest) on ice using a sonifier (Bandelin Sonopuls, Berlin, Germany). After complete disruption, cell debris was removed by centrifugation (11,000 g, 45 min, 4 °C). The resulting supernatant was further processed, by either using Ni-NTA spin columns, following the instruction of the manufacturer (Qiagen, Venlo, Netherlands) or by using a 5 mL HisTrap column (GE-Healthcare). The HisTrap columns were equilibrated with 5 column volumes (CV) lysis-buffer and then loaded with the supernatant, washed twice with 5 CV lysis buffer and eluted with an increasing imidazole concentration from 20 mM imidazole (lysis-buffer) to 500 mM imidazole (elution-buffer, 50 mM phosphate, 300 mM NaCl, 500 mM imidazole, pH 7.5). Fractions with purified CaeEnR1 were analyzed via SDS-PAGE, concentrated and rebuffed with Amicon® Ultra 4 mL centrifugal filters (Merck KGaA, Darmstadt, Germany). Protein concentration was photometrically determined by using the 260/280 ratio and the specific extinction coefficient ($E_{280} = 40340 \text{ M}^{-1}\cdot\text{cm}^{-1}$), calculated with the ExPASy ProtParam tool.^[29]

Enzyme assay

UV method: CaeEnR1 activity was determined by recording the oxidation of NADH/NADPH at 340 nm ($E_{340} = 6620 \text{ M}^{-1}\cdot\text{cm}^{-1}$) on a Nanophotometer (Implen, Munich, Germany). The typical reaction mixture contained 0.2 mM NADPH, 0.2 mM substrate and an appropriate amount of enzyme in a total volume of 1 mL. For pH dependency, the mixture was incubated in either 50 mM acetate buffer (pH 4.5–6.0), 50 mM phosphate buffer (pH 6.5–8.0) or 50 mM borate buffer (pH 8.5–10.0) to determine the pH-optimum. Effects of the temperature were measured by incubating the reaction mixture at different temperatures, ranging from 4 °C–50 °C. One unit of enzyme activity was defined as the conversion of μmol substrate per minute.

GC-MS method: A typical reaction mixture of 1 mL contained 0.2 mM NADPH, 0.1 mM substrate, an appropriate amount of enzyme in 50 mM phosphate buffer, pH 7.5. The mixture was incubated at 24 °C for 3 h.

Preparative scale biotransformation

Biotransformation in a preparative scale contained 25 mM of substrate **1** (solved in ethanol, 10% final solvent concentration), 0.1 mM NADP^+ , 100 mM glucose, 100 U glucose dehydrogenase from *Pseudomonas* sp. (Sigma Aldrich) and an appropriate amount enzyme in 50 mM phosphate buffer, pH 7.5 with a final volume of 100 mL. The mixture was incubated for 16 h at 24 °C. After defined times (1 h, 3 h, 6 h and 16 h) an aliquot was taken to monitor the reaction progress.

Kinetic parameters

Steady-state kinetic parameters were calculated by incubating purified CaeEnR1 with different concentrations according to the used substrates ranging from 7.5–300 μM and 0.2 mM NADPH. Resulting data was fitted with the Michaelis-Menten equation in OriginPro 2018 software.

Product analysis

The reaction products were extracted with 400 μL ethyl acetate, followed by mixing on a vortexer and centrifugation for 2 min at 13000 g. Analysis of the reaction products in the organic layer was carried out on a Agilent Technologies 7890 A GC-MS-system (Santa Clara, USA), equipped with a VFWax column (30 m \times 0.25 mm \times 0.25 μm film thickness, Santa Clara, USA) operated in splitless mode under the following parameters: carrier gas, Helium with a constant flow of 1.2 $\text{mL}\cdot\text{min}^{-1}$. Oven temperature was at 40 °C (3 min), 10 °C $\cdot\text{min}^{-1}$ to 240 °C and hold for 7 min. The mass spectrometer operated in electron impact mode with an electron energy of 70 eV and scanned in a range of m/z 33–300. Conversion rates were calculated by using the peak areas. Retention times and mass spectrum was compared with authentic standards, the NIST database or by the characteristic fragmentation pattern and molecule ion.

In silico analysis of CaeEnR1

Phylogenetic analysis and amino acid alignments: Sequences for phylogenetic analysis and sequence alignments were obtained via the National Center of Biotechnology Information (NCBI, <https://www.ncbi.nlm.nih.gov/>). Amino acid alignments and tree building were performed with the Clustal Omega web tool (<https://www.ebi.ac.uk/Tools/msa/clustalo/>). Visualization of the phylogenetic tree was carried out via the online tools, interactive tree of life (iTOL, <https://itol.embl.de/>) and <http://www.phylogeny.fr>.

Acknowledgements

We gratefully acknowledge the financial support by the Deutsche Forschungsgemeinschaft (DFG, German Research Foundation)-Funder Id: <https://doi.org/10.13039/501100001659>, Grant Number: RU 2137/1-1. Open access funding enabled and organized by Projekt DEAL.

Conflict of Interest

The authors declare no conflict of interest.

Keywords: ene-reductase • biocatalysis • regioselectivity • double bond reductase • alkynes

- [1] R. A. Sheldon, J. M. Woodly, *Chem. Rev.* **2018**, *118*, 801–838.
- [2] M. C. Bryan, P. J. Dunn, D. Entwistle, F. Gallou, S. G. Koenig, J. D. Hayler, M. R. Hickey, S. Hughes, M. E. Kopach, G. Moine, P. Richardson, F. Roschangar, A. Steven, F. J. Weiberth, *Green Chem.* **2018**, *20*, 5082–5103.
- [3] H. S. Toogood, N. S. Scrutton, *ACS Catal.* **2018**, *8*, 3532–3549.
- [4] B. Youn, S.-J. Kim, S. G. A. Moinuddin, C. Lee, D. L. Bedgar, A. R. Harper, L. B. Davin, N. G. Lewis, C. Kang, *J. Biol. Chem.* **2006**, *281*, 40076–40088.

- [5] J. Mano, Y. Torii, S. Hayashi, K. Takimoto, K. Matsui, D. Inzé, E. Babychuk, S. Kushnir, K. Asada, *Plant Cell Physiol.* **2002**, *43*, 1445–1455.
- [6] P. C. Guo, P. X. X. Ma, Z. Z. Bao, J. D. Ma, Y. Chen, C. Z. Zhou, *J. Struct. Biol.* **2011**, *176*, 112–118.
- [7] D. Karrer, M. Rühl, *PLoS One* **2019**, e0218625.
- [8] Y.-J. Liu, X.-Q. Pei, H. Lin, P. Gai, Y.-C. Liu, Z.-L. Wu, *Appl. Microbiol. Biotechnol.* **2012**, *95*, 635–645.
- [9] S. Raimondi, D. Romano, A. Amaretti, F. Molinari, M. Rossi, *J. Biotechnol.* **2011**, *156*, 279–285.
- [10] Y. Fu, K. Castiglione, D. Weuster-Botz, *Biotechnol. Bioeng.* **2013**, *110*, 1293–1301.
- [11] R. A. Sheldon, D. Brady, *ChemSusChem* **2019**, *12*, 2859–2881.
- [12] R. Shen, T. Chen, Y. Zhao, R. Qiu, X. Zhou, S. Yin, X. Wang, M. Goto, L. B. Han, *J. Am. Chem. Soc.* **2011**, *133*, 17037–17044.
- [13] A. Mori, Y. Miyakawa, E. Ohashi, T. Haga, T. Maegawa, H. Sajiki, *Org. Lett.* **2006**, *8*, 3279–3281.
- [14] L. Longwitz, T. Werner, *Angew. Chem. Int. Ed.* **2020**, *132*, 2792–2785.
- [15] Y. Wang, Z. Huang, X. Leng, H. Zhu, G. Liu, Z. Huang, *J. Am. Chem. Soc.* **2018**, *140*, 4417–4429.
- [16] I. Schnetmann-Göttker, P. White, M. Brookhart, *J. Am. Chem. Soc.* **2003**, *126*, 1804–1811.
- [17] M. Gupta, C. Hagen, W. C. Kaska, R. E. Cramer, C. M. Jensen, *J. Am. Chem. Soc.* **1997**, *119*, 840–841.
- [18] H. Kasahara, Y. Jiao, D. L. Bedgar, S.-J. Kim, A. M. Patten, Z.-Q. Xia, L. B. Davin, N. G. Lewis, *Phytochemistry* **2006**, *67*, 1765–1780.
- [19] K. L. Ringer, M. E. McConkey, E. M. Davis, G. W. Rushing, R. Croteau, *Arch. Biochem.* **2003**, *418*, 80–92.
- [20] D. J. Mansell, H. S. Toogood, J. Waller, J. M. X. Hughes, C. W. Levy, J. Gardiner, N. S. Scrutton, *ACS Catal.* **2013**, *3*, 370–379.
- [21] A. Skrobiszewski, R. Ogórek, E. Płaskowska, W. Gładkowski, *Biocatal. Agric. Biotechnol.* **2013**, *2*, 26–31.
- [22] A. Romagnolo, F. Spina, E. Brenna, M. Crotti, F. Parmeggiani, G. C. Varese, *Fungal Biol. Rev.* **2015**, *119*, 487–493.
- [23] K. Yamamoto, Y. Oku, A. Ina, A. Izumi, M. Doya, S. Ebata, Y. Asano, *ChemCatChem* **2017**, *9*, 3697–3704.
- [24] Y. Wang, Z. Huang, X. Leng, H. Zhu, G. Liu, Z. Huang, *Appl. Microbiol. Biotechnol.* **2014**, *98*, 705–715.
- [25] J. Mano, E. Babychuk, E. Belles-Boix, J. Hiratake, A. Kimura, D. Inzé, S. Kushnir, K. Asada, *Eur. J. Biochem.* **2000**, *267*, 3661–3671.
- [26] A. Müller, R. Stürmer, B. Hauer, B. Rosche, *Angew. Chem. Int. Ed.* **2007**, *46*, 3316–3318; *Angew. Chem.* **2007**, *119*, 3380–3382.
- [27] Y. Wu, Y. Cai, Y. Sun, R. Xu, H. Yu, X. Han, H. Lou, A. Cheng, *FEBS Lett.* **2013**, *587*, 3122–3128.
- [28] K. F. Biegasiewicz, S. J. Cooper, M. A. Emmanuel, D. C. Miller, T. K. Hyster, *Nature* **2018**, *10*, 770–775.
- [29] E. Gasteiger, C. Hoogland, A. Gattiker, S. Duvaud, M. R. Wilkins, R. D. Appel, A. Bairoch, *The Proteomics Protocols Handbook* (Ed.: John M. Walker), Humana Press, **2005**, pp. 571–607.
- [30] F. R. Schmidt, *Appl. Microbiol. Biotechnol.* **2005**, *68*, 425–435.
- [31] D. Vasić-Rački, Z. Findrik, A. Vrsalović Presečki, *Appl. Microbiol. Biotechnol.* **2011**, *91*, 845–856.

Manuscript received: December 18, 2020
Revised manuscript received: January 22, 2021
Accepted manuscript online: February 1, 2021
Version of record online: February 19, 2021